SECTION 3: RESULTS OF WORK PERFORMED

Gas Holdup*

Tarrer et al. (8) examined the general applicability of two gas holdup correlations in bubble columns in conjunction with a dispersion model for the solvent-refined coal process. One correlation was that of Hikita and Kikukawa (9), who proposed the expression

$$\epsilon_g = 0.505\ V_g^{0.42} (72/\sigma)^{2/3}\ (1/\mu)^{0.05} \qquad (1)$$

The other correlation was that of Yoshida and Akita (10) who expressed the gas void fraction as a complex function of three dimensionless functional groups:

$$\frac{\epsilon_g}{(1 - \epsilon_g)^4} = C_1\ (N_{Bo})^{1/8}\ (N_{Ga})^{1/12}\ (N_{Fr}) \qquad (2)$$

where

$$N_{Bo} = gD^2\ \rho_L/\sigma \qquad \text{(Bond number)} \qquad (3)$$

$$N_{Ga} = gD^3/\nu_L^2 \qquad \text{(Galileo number)} \qquad (4)$$

$$N_{Fr} = V_g/\sqrt{gD} \qquad \text{(Froude number)} \qquad (5)$$

---

*The gas holdup work carried out at Air Products in support of dissolver cold-flow modelling studies was summarized in a published I&EC paper titled, "Gas Holdup in Gas-Liquid and Gas-Liquid-Solid Flow Reactors" by D. H. S. Ying (15). The following results have been extracted in their entirety from this publication.

and C_1 = 0.20 for nonelectrolyte solution and C_1 = 0.25 for electrolyte solution.

Equation (2) also predicts a holdup independent of column diameter, and it may be written in terms of only two dimensionless groups, such as

$$\frac{\epsilon_g}{(1-\epsilon_g)^4} = C_1 \left(\frac{\rho_L^3 \nu_L^4 g}{\sigma^3}\right)^{1/24} \left(\frac{V_g^3}{g\nu_L}\right)^{1/3} \qquad (6)$$

Tarrer et al. arrived at the general conclusion that eqn. (2) should be used when column diameter (D) is greater than 5.9 in., while an average of eqn. (1) and (2) was recommended for design purposes when D is less than 5.9 in.

Gas holdup data in the water/nitrogen system are shown in Figure 3. Excellent agreement was obtained between Yoshida's correlation and the results from the 5-in.-diam column. The results from the 2-in.-diam column also show good agreement at low gas input rates, but significant deviations were observed at superficial velocities above 0.10 ft/sec. At this gas input rate, fully developed slug flow was observed in the 2-in.-diam column. In the 5-in.-diam column, slug flow behavior was not seen up to the maximum superficial velocity of 0.27 ft/sec attainable with the equipment.

The gas void fraction predicted by the correlation of Hikita and Kikukawa (eqn. 1) was always higher than the experimental results from both columns at low superficial gas velocities, as shown in Figure 3. The prediction from eqn. 1 apparently approaches measured gas holdup results (5-in.-diam column)

FIGURE 3

GAS HOLDUP IN WATER/NITROGEN SYSTEM

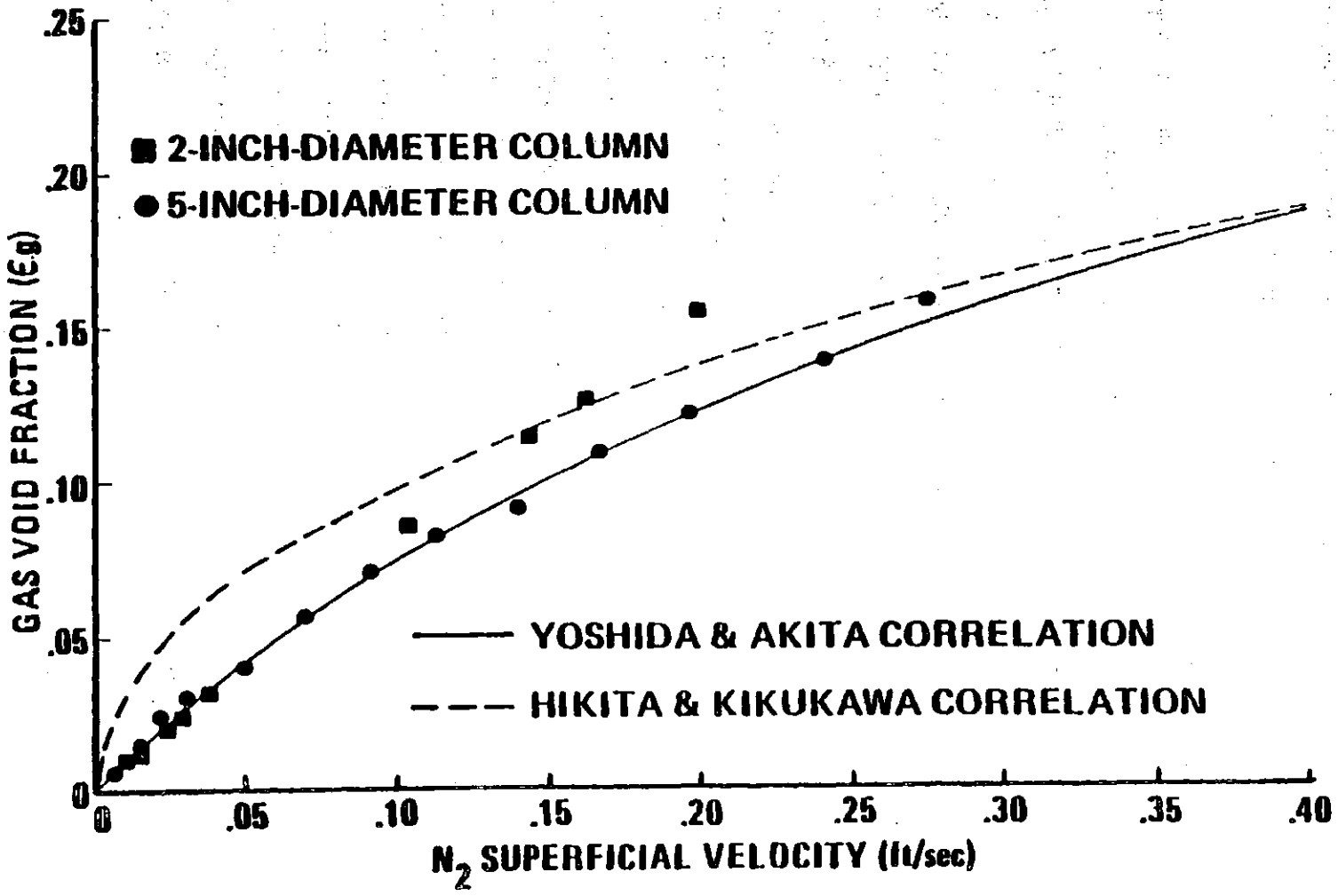

at higher gas superficial velocities. However, as mentioned by Tarrer et al., the application of eqn. 1 becomes limited at high gas superficial velocities, since it predicts a gas void fraction greater than unity.

The methanol/nitrogen system showed similar behavior, as shown in Figure 4. The average bubble size is smaller in methanol than in water because of the lower surface tension of methanol, resulting in a slightly larger gas holdup. The deviation between the gas holdup measured from the 2- and 5-in.-diam columns is less in the methanol/nitrogen system, presumably because the wall proximity effect is lower for small bubbles than for larger ones. Yoshida's correlation shows reasonably good agreement with the methanol/nitrogen gas holdup results. However, the prediction from eqn. (1) is much too high. Since the small dependence on the liquid viscosity shown in eqn. (1) has negligible impact on the gas holdup, the dependence on the liquid surface tension must be responsible for this high gas holdup prediction. The correlation of Yoshida and Akita, on the other hand, appears to handle the effect of surface tension very well, since it is very close to the experimental data for both water/nitrogen and methanol/nitrogen systems. This suggests the general application of Yoshida's correlation for low surface tension systems. In addition, the correlation of Yoshida and Akita correctly predicts that at low gas flow rates, the bubble rise velocity is independent of superficial gas velocity. This is more obvious when eqn. (6) is rearranged to give an explicit expression for the bubble rise velocity (V_{BR}) as $\epsilon_g \ll 1$:

$$\frac{V_{BR}}{(g\,\nu_L)^{1/3}} = \frac{1}{C_1}\left(\frac{\sigma^3}{\rho_L^3 \nu_L^4 g}\right)^{1/24} \qquad (7)$$

FIGURE 4

GAS HOLDUP IN METHANOL/NITROGEN SYSTEM

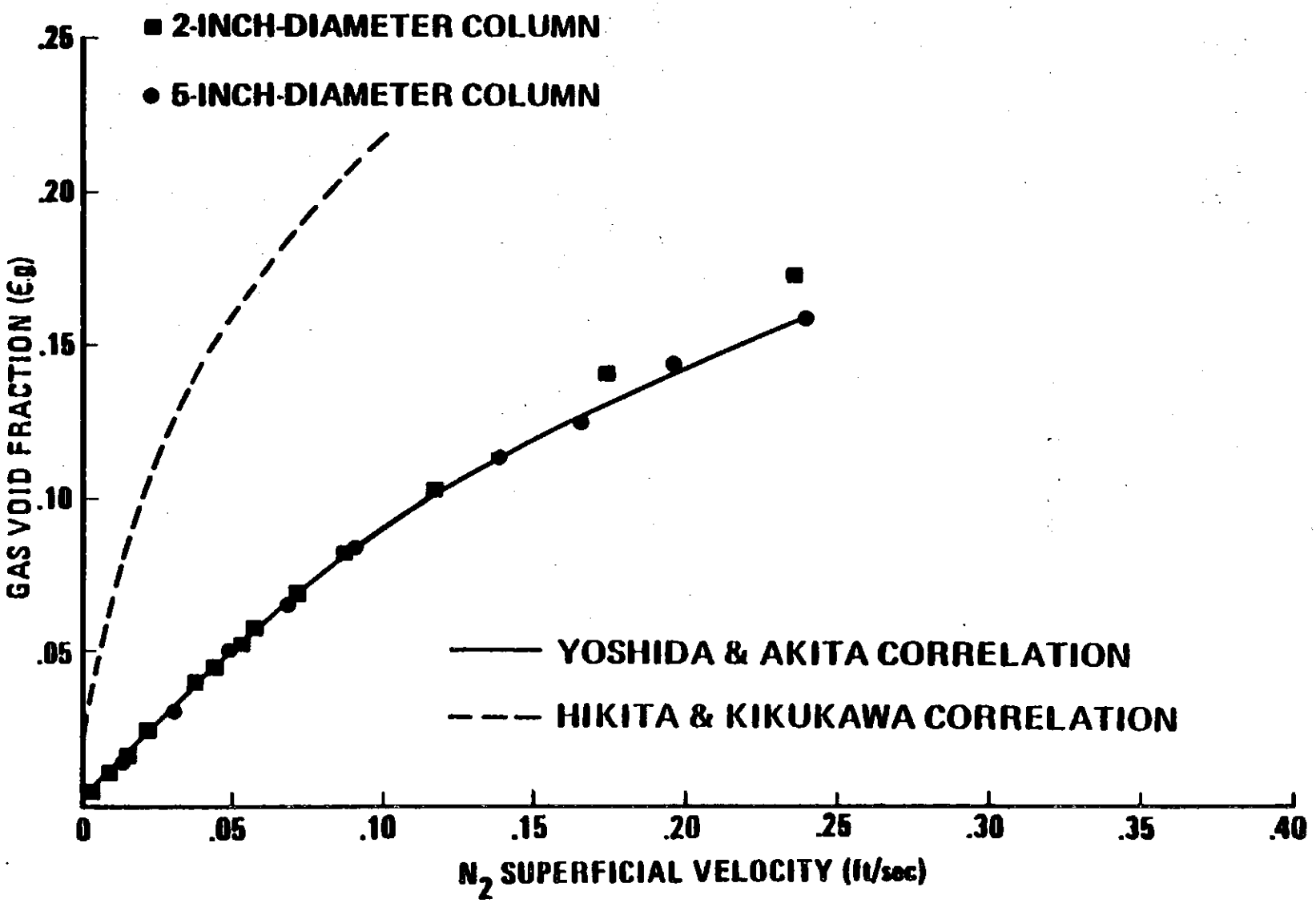

where $V_{BR} = V_g/\varepsilon_g$. Substitution of the physical properties of water gives V_{BR} a value of 1 ft/sec, which approximates the terminal velocity of single bubbles in water (11).

Tarrer et al. have recommended an average of eqn. (1) and (2) for design purposes when the column diameter is less than 5.9 in. However, it was found that an average of these two equations does not fit the data from the 5-in.-diam column as well as does eqn. (2) alone. In fact, the correlation of Hikita and Kikukawa is not dimensionless, making it difficult to scale-up bench-scale data.

When a distributor plate with seven 0.25-in. openings was used in the 5-in. diameter column, the measured gas holdup in water was identical to that obtained without the plate at gas velocities up to 0.09 ft/sec. At higher gas input rates, gas was trapped below the distributor plate. This extra gas pocket displaced more fluid, causing an apparently larger gas void fraction. After correcting for this gas pocket effect, the gas void fraction at high gas input rates (Figure 5) agreed with those without the distributor plate (Figure 3). This agreement shows that the presence of a distributor plate does not affect gas holdup in the section of the bubble column above the plate.

The presence of suspended solid particles in a bubble column reduced gas holdup. This effect was somewhat dependent on the column diameter. The difference between gas holdup in a 2-in.-diam column with and without suspended solids (-140 mesh) was negligible (Figure 6). When the column

FIGURE 5

EFFECT OF DISTRIBUTOR PLATE ON GAS HOLDUP IN 5-INCH DIAMETER COLUMN (WATER/NITROGEN)

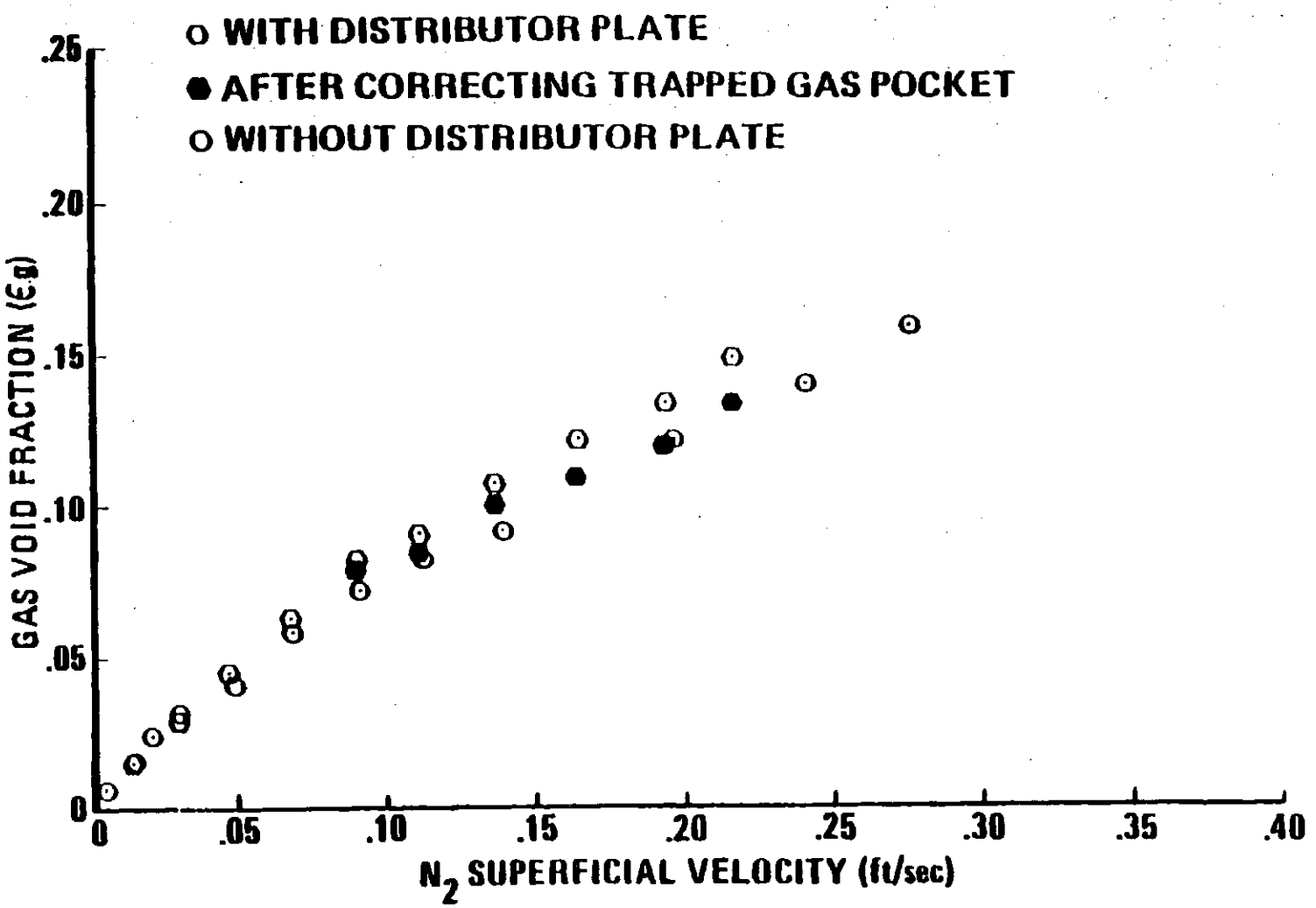

FIGURE 6

EFFECT OF SOLIDS ON GAS HOLDUP IN A 2-INCH DIAMETER COLUMN

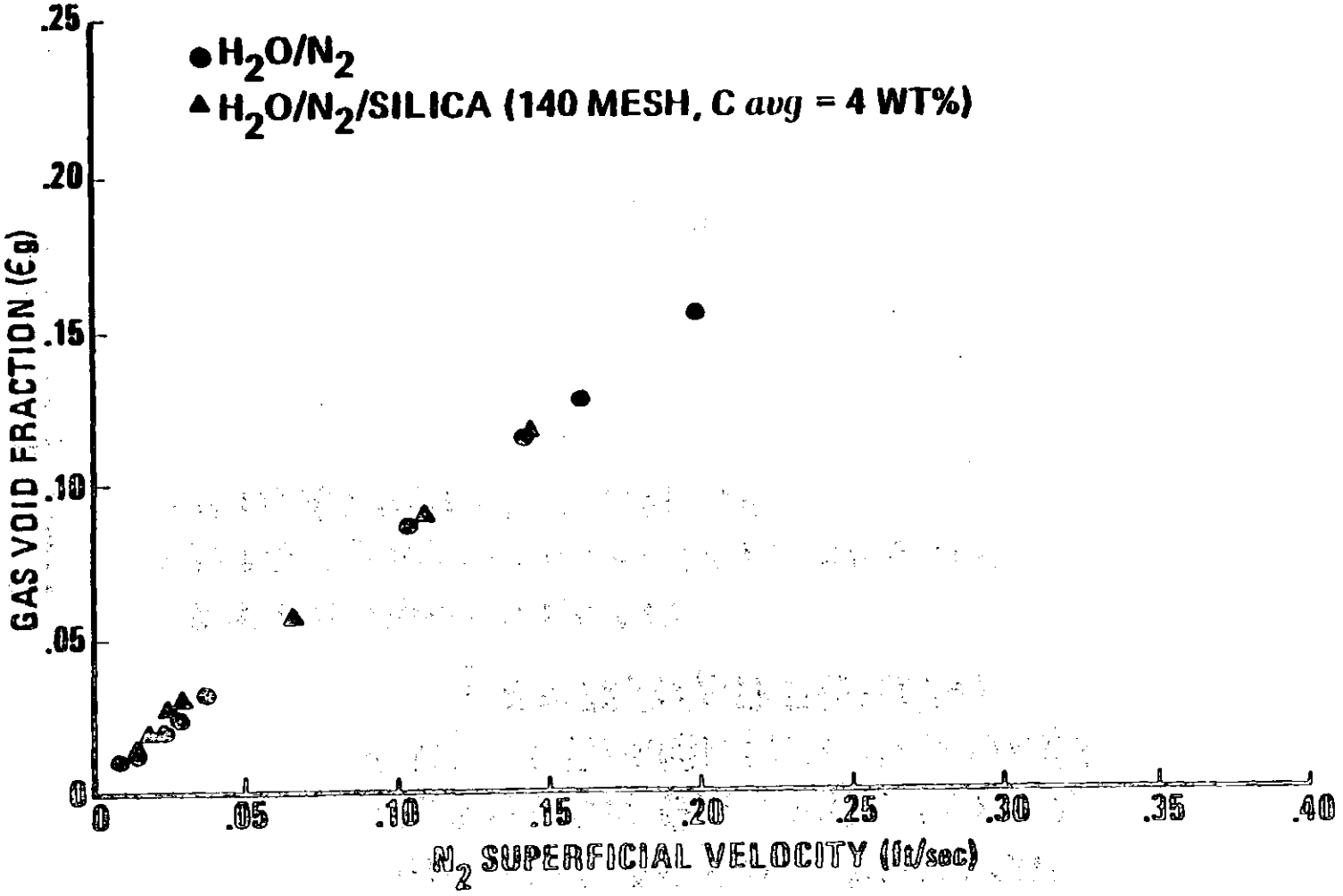

diameter was increased to 5 in., less gas holdup was observed in the presence of the suspended solids (-140 mesh), as shown in Figure 7. A gas holdup study with air-water-glass spheres by Kato et al. (12) showed similar results. They observed higher rising velocity of the coalesced bubbles in the presence of solid particles. In this system, the suspended silica particles made the slurry column opaque, and observation of bubble size and rising velocity was not possible. In any event, the difference in gas holdup is less obvious at high gas flow rates. This also agrees with the observation of Kato et al. (12), and it suggests that high gas turbulence reduces the coalescence effect caused by the presence of suspended solid. An identical reduction effect at low superficial gas velocities was observed when larger particles (30-45 mesh) were used in the 5-in.-diam column. With these larger particles, larger coalesced bubbles were observed, and the reduction effect extended to slightly higher gas input rates (0.19 vs. 0.13 ft/sec), as shown in Figure 8. This suggests that the gas turbulence required to reduce the coalescence effect is higher for larger solid particles. Increasing the average solids concentration from 15.7 to 45.0 wt % produced no further systematic change in gas holdup, as shown by Figure 7.

Gas holdup data from the 5-in.-diam column with suspended solid particles showed that gas holdup is not affected by the slurry flow rate. Three different slurry input rates ranging from 5 to 25 cm^3/sec were employed. The results showed negligible differences between the gas holdups with and without slurry flow.

FIGURE 7

EFFECT OF SOLID CONCENTRATION ON GAS HOLDUP IN A 5-INCH DIAMETER COLUMN

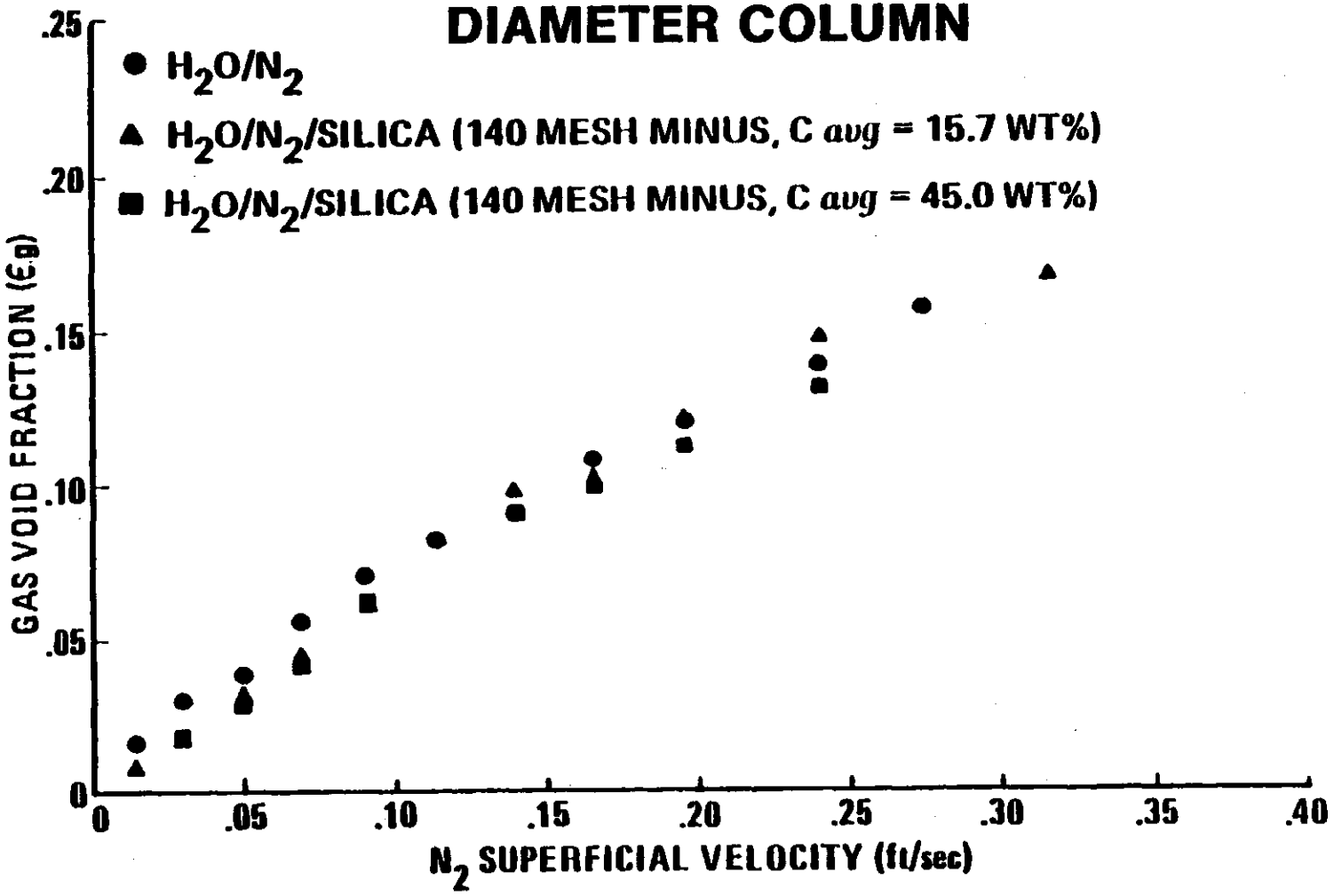

FIGURE 8

EFFECT OF LARGE SOLID PARTICLES (30–45 MESH) ON GAS HOLDUP IN A 5-INCH DIAM. COLUMN

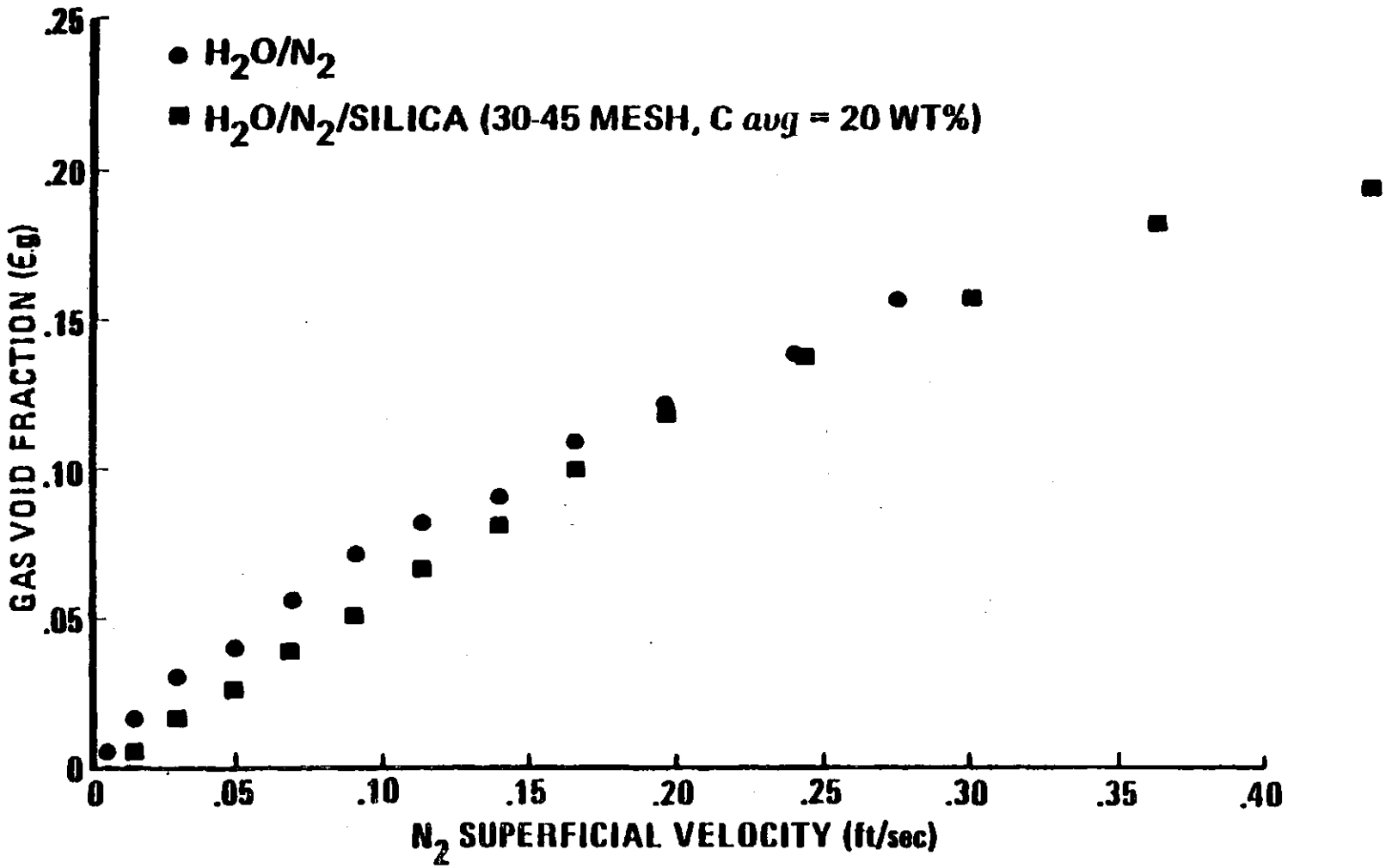

The entrance effect on gas holdup was studied in the 5-in.-i.d. column using a 0.25-in.-diam single orifice inlet and three porous metal plates with 40-, 60-, and 100-micron openings. The results for the 100-micron opening plate are compared with the single inlet in Figure 9 for a water/air(N_2) system. They show a significant increase in gas holdup for the porous plate inlet over the single inlet at the same gas superficial velocities. Similar tests with a kerosene/nitrogen system also showed a significant increase in gas holdup for the porous plate inlet. Extensive foaming in this system resulted in even higher gas holdup than did the water/air(N_2) system. However, from observation of nonfoaming water/air(N_2) systems, it may be concluded that the porous plate inlet results in higher gas holdup than does a single inlet; this dramatic increase may be attributable to the extremely fine gas bubbles generated by the porous plate.

Gas holdup tests with the 40- and 60-micron opening porous plates revealed that gas holdup increases with decreasing pore size. Observation revealed that, along with the increase in gas holdup, bubble size decreased with decreasing pore size.

The gas holdup results in the presence of solid particles with the porous metal plate inlet are also shown in Figure 9. The 40-60 mesh sand particles (~14 wt %) settled on the porous plate and totally suppressed the formation of fine bubbles, which drastically reduced gas holdup. However, tests with finer size particles in the kerosene/nitrogen system showed a very small reduction in gas holdup due to the presence of solids if the particles were

FIGURE 9

EFFECT OF POROUS PLATE GAS INLET ON GAS HOLDUP WITH AND WITHOUT SOLID PRESENT IN 5-INCH DIAM. COLUMN

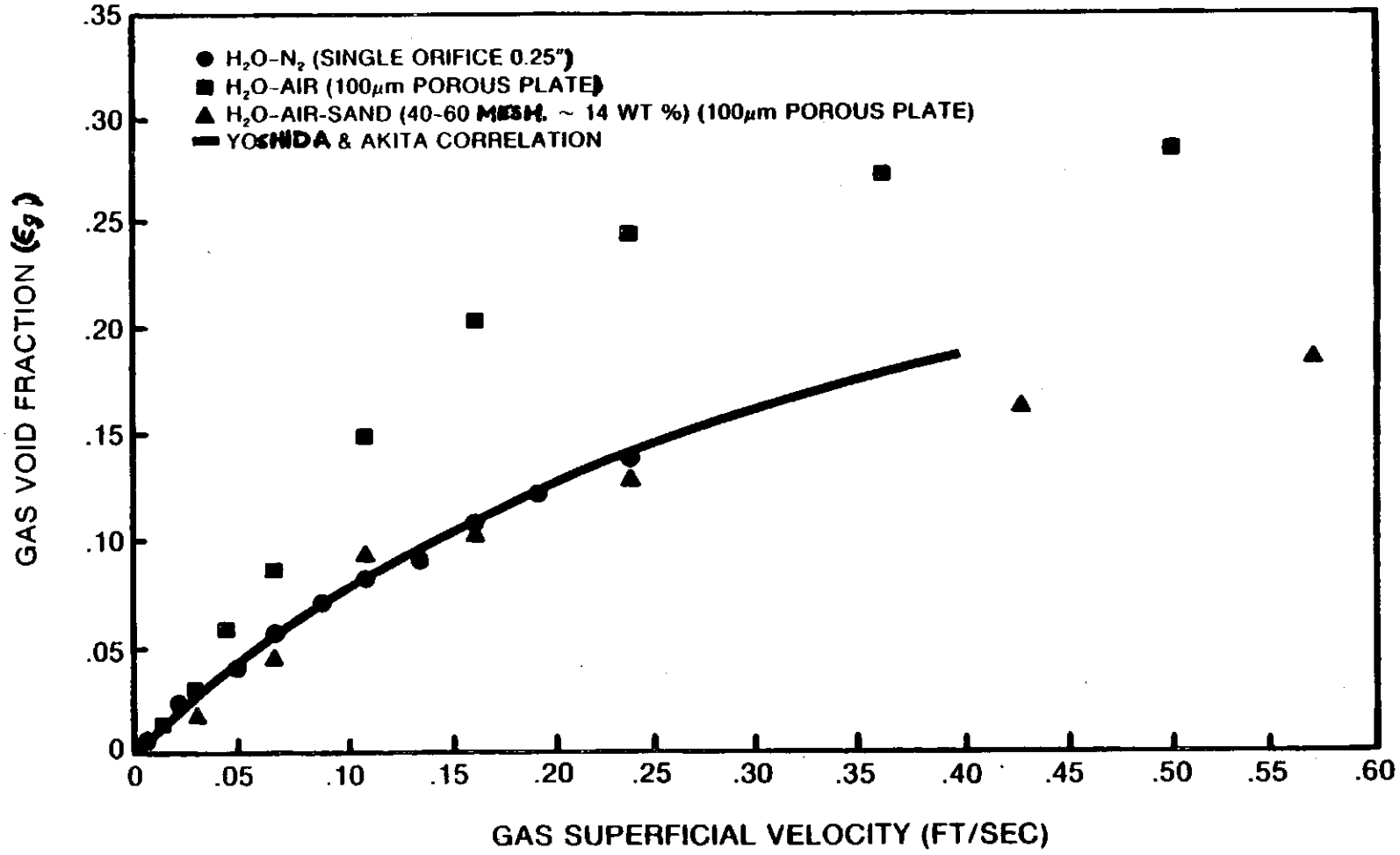

fully suspended. The significance of this study is that it demonstrates the important role of particles in altering the characteristics of the inlet, which governs the gas holdup.

Critical Gas Velocity

Critical gas velocity measurements were carried out in the 5-in.-diam column using a nitrogen-water-silica system. The effect of several different variables on critical gas velocity such as particle size, fluid flow, solids concentration, and liquid and gas properties were studied in detail and the results are summarized below:

(a) Effect of Particle Size

To study the effect of particle size on critical gas velocity, sand particles ranging in size from 80 to 20 mesh were used. The particles were arbitrarily divided into four groups, as shown below:

60 mesh	$\geq$	Group I	>	80 mesh
45 mesh	$\geq$	Group II	>	60 mesh
30 mesh	$\geq$	Group III	>	45 mesh
20 mesh	$\geq$	Group IV	>	30 mesh

The critical gas velocity measurements are provided in Table 2. When gas velocity dropped below the critical value, sand particles were observed to settle at the bottom, with the gas channeling through the settled solid bed. The amount of settled solid decreased with increasing gas

Table 2

Effect of Particle Size on Critical Gas Velocity

Group no.	Particle size range		Critical gas velocity range (ft/sec)
	Mesh	Micron (μm)	
I	60-80	250-177	0.193 - 0.217
II	45-60	354-250	0.298 - 0.362
III	30-45	595-354	0.462 - 0.503
IV	20-30	841-595	No full suspension to 0.57 ft/sec

Table 3

Particle Settling Velocities in Infinite Media

Mesh number	Diameter (μm)	Settling velocity (ft/sec)		
		Ethanol	Water	Ethanol-water[a]
80	177		0.0567	
60	250		0.0971	
45	354		0.1535	
30	595	0.24	0.2592	0.13
20	841		0.3707	

[a] 30 wt % ethanol-
70 wt % water

velocity. As the critical gas velocity was reached, the momentum transferred from the gas phase was large enough to suspend all the sand particles. The sieve opening (in microns) for each particle range is shown in Table 2. With the assumptions of spherical particles and the same diameter as the sieve opening, the settling velocities of sand particles were calculated based upon particle drag in three infinite media, as shown in Table 3. It is reasonable to assume that the largest particle in each group governs the critical gas velocity, as shown in Table 2. It is then interesting to note from Tables 2 and 3 that the critical gas velocity in each group is approximately twice the settling velocity of the largest particle of the corresponding group. By extrapolating these results, the Group IV particles (20-30 mesh) are predicted to have a critical gas velocity of about 0.74 ft/sec, which was not achievable in the current program due to equipment limitations.

(b) Effect of Solids Concentration

The effect of solids concentration on critical gas velocity was studied with 80-120-mesh silica particles. By raising the average solids concentration from 20 to 36 wt %, critical gas velocity was increased by 0.012 ft/sec. A further increment of the average concentration from 36 to 59 wt % increased critical gas velocity by another 0.013 ft/sec. However, at a solids concentration of 20 wt %, the span of critical gas velocity, which ranged from 0.137 to 0.165 ft/sec, was compatible with these increases, suggesting that the slight dependence on solids concentration was not very significant. A test involving halving the

amount of solids while maintaining the same concentration revealed that critical gas velocity is not dependent on the absolute amount of solids present. It was concluded that critical gas velocity is slightly dependent on solids concentration.

(c) Effect of Liquid Properties

The effect of liquid properties on critical gas velocities was determined using three liquids whose physical properties are given in Table 4. The critical gas velocity measurements are provided in Table 5. When the mixture of ethanol and water was used, the critical gas velocities for Groups II and V were reduced by approximately 30% of those measured in pure water. Examination of the physical properties of these two solutions (Table 4) reveals two possible causes for this reduction, namely surface tension and viscosity. However, the experiment with pure ethanol eliminated the possibility of a surface tension effect. The surface tension of the mixed solution (37.43 dynes/cm) was more than a factor of two lower than that of pure water. If surface tension were responsible for the observed reduction in critical gas velocity in the mixture, then pure ethanol, which has a surface tension (22.75 dynes/cm) lower than that of the mixture, would show a similar reduction. Surprisingly, the critical gas velocities for the 80-120 mesh particles (Group II) in pure ethanol were indistinguishable from those observed in pure water (Table 5). Hence, liquid surface tension is not responsible for the reduction observed in the mixture, thereby leaving liquid viscosity as the sole explanation. The solids settling velocity was lower in the mixed solution than in pure water. By calculation, the

Table 4

Physical Properties of Various Liquids Used

in The Critical Gas Velocity Experiments

Liquid	Physical properties		
	Surface tension (dynes/cm)	Viscosity (cP)	Density (g/cm^3)
Water	72.8	1.0	1.000
30 wt % ethanol-70 wt % water	37.43	3.2	0.9556
Ethanol	22.75	1.2	0.7893

Table 5

Effects of Particle Size and Liquid Properties on Critical Gas Velocities

Group no.	Particle size		Critical gas velocity (ft/sec)		
	mesh	μm	Water	Ethanol-water[a]	Ethanol
I	140 minus	less than 105	0.013	---	---
II	80-120	177-125	0.137-0.165	0.10-0.11	0.137-0.165
III	60-80	250-177	0.193-0.217	---	---
IV	45-60	354-250	0.298-0.362	---	---
V	30-45	595-354	0.482-0.503	0.344	---
VI	20-30	841-595	No full suspension to 0.57 ft/sec	---	---

[a]30 wt % ethanol
-70 wt % water

settling velocities of a 30-mesh (595-μm) particle in the mixed solution and in the pure ethanol were found to be 0.13 and 0.24 ft/sec, respectively. The insignificant difference between pure ethanol (0.24 ft/sec) and pure water (0.2592 ft/sec) clearly explains the indistinguishable critical gas velocities measured in those two solutions. On the other hand, a twofold difference in the settling velocities of the 30-mesh particles in mixed solution and pure water (Table 3) explain the observed reduction in critical gas velocity. This also agrees with the findings on particle size effect, which showed that critical gas velocity increased with increasing particle settling velocity.

(d) Effect of Gas Properties

This effect was investigated using Freon 12 gas for the 80-120-mesh silica particles. This heavier gas (0.318 lbm/ft^3) showed no prominent change from the nitrogen gas (0.078 lbm/ft^3), which is lighter by a factor of four. That a fourfold increase in gas density produced no change in the critical gas velocity suggests that critical gas velocity is probably independent of gas density.

Solids Accumulation

Solids buildup in vertical tubular reactors can be generally split into two classes: settled solids and suspended solids. Settled solids represent deposits typically formed at the bottom of the column. Suspended solids refer to accumulated solids in the turbulent phase along the axial dimension. Both types of accumulation were encountered in studies with the 2-in.-i.d. column.

The conical bottom design of the 5-in.-i.d. column completely eliminates the settled solids deposit problem. However, the 2-in.-i.d. column with cylindrically shaped bottom always contains settled solids, regardless of the level of turbulence introduced by the gas flowing through the slurry phase.

The problem of suspended solids accumulation was studied in greater detail than was settled solids buildup because the latter can be eliminated by proper bottom design. A theoretical model developed by Cova (13) to predict the solids profile in a reactor was used to compare results from this study. The model describes the solids motion by superimposing diffusion on the bulk flow. Several assumptions were made in applying the model to simulate the solid accumulation results in the 5-in.-i.d. column: (a) the time-dependent portion of the solution was position-independent, (b) dispersion coefficients between the liquid and gas phases were similar, and (c) the Stoke's Law was applicable to estimate the settling velocity of the solid particles to compute the solids concentration of the exiting stream at different slurry input rates.

The effect of slurry flow rate on solids accumulation is more dramatic without gas flow than with gas bubbling through the column. The solids concentration of the slurry exiting the 5-in.-diam column at three different slurry feed rates (no gas input) versus time is shown in Figure 10. The feed concentration varied from 7.5 to 8.1 wt %. The results indicate a large enhancement in the solids concentration in the exiting stream as the slurry input rate was increased. The comparison of these experimental data with the theoretical predictions based on the feed solid particle size distribution are shown in Figures 11 through 13. The good agreement suggests the validity of

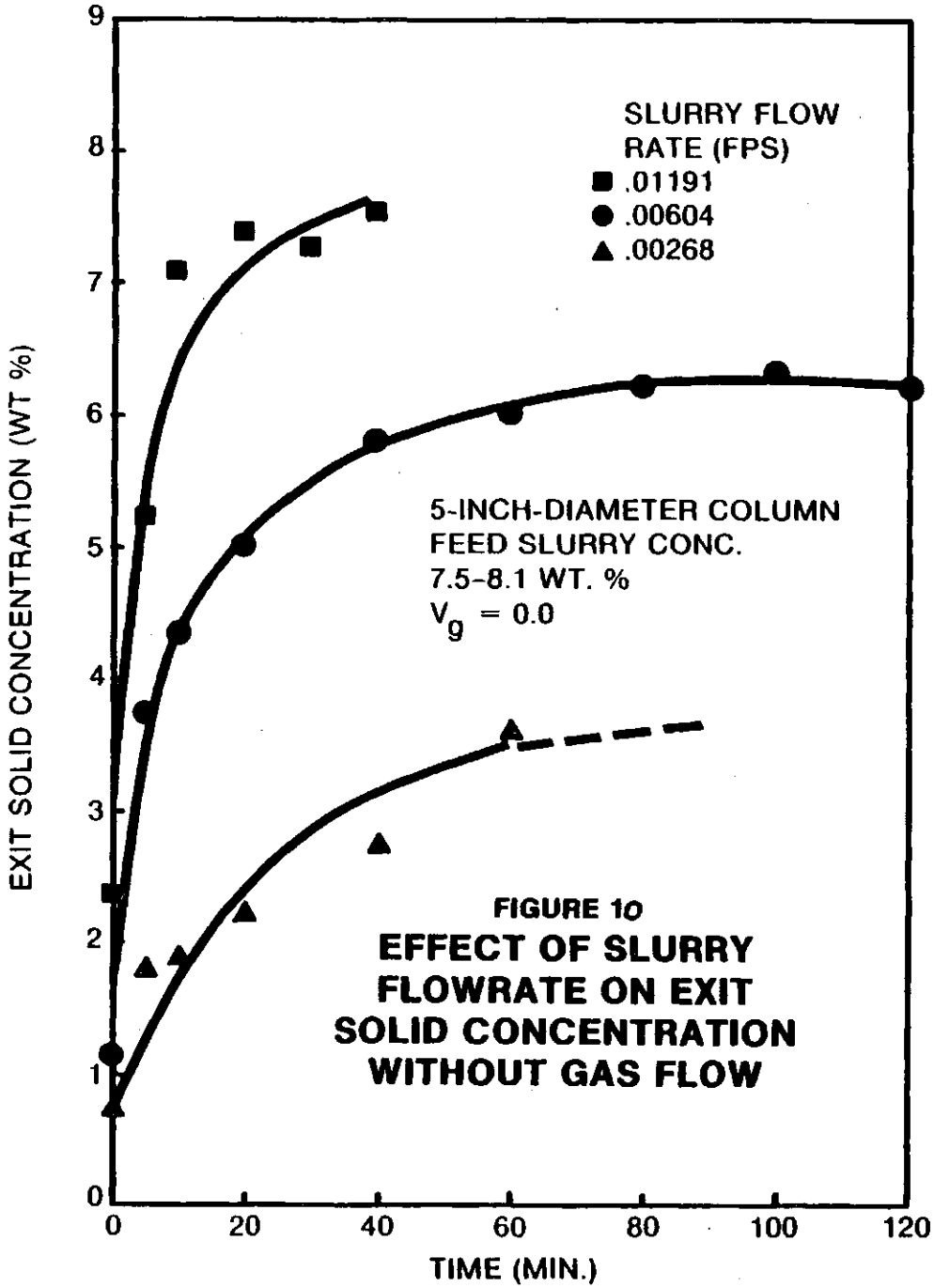

FIGURE 10

EFFECT OF SLURRY FLOWRATE ON EXIT SOLID CONCENTRATION WITHOUT GAS FLOW

FIGURE 11

EXIT SOLID CONCENTRATION VERSUS TIME SHOWING COMPARISON WITH THE MODEL BASED ON SIZE DISTRIBUTION (NO GAS FLOW)

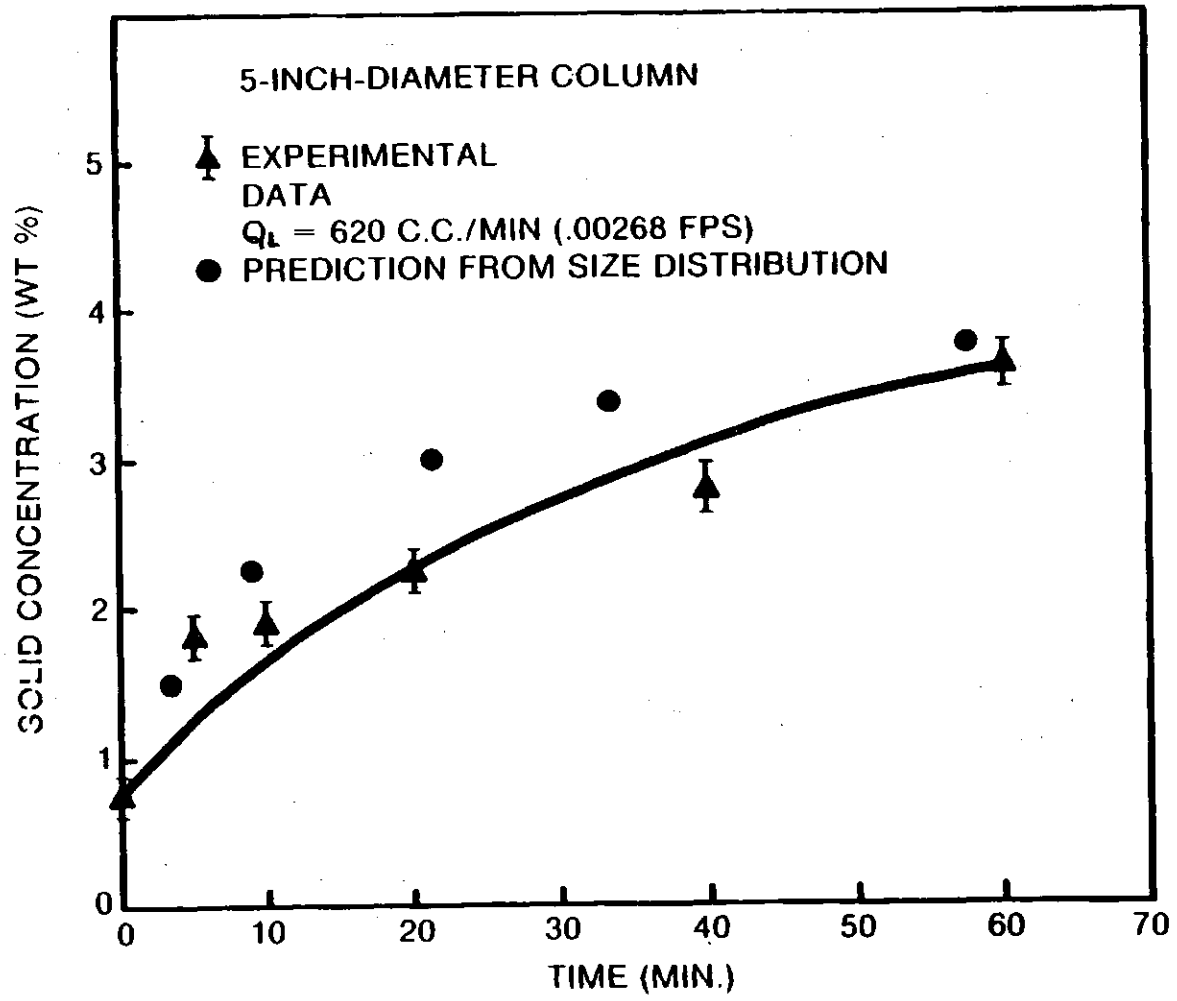

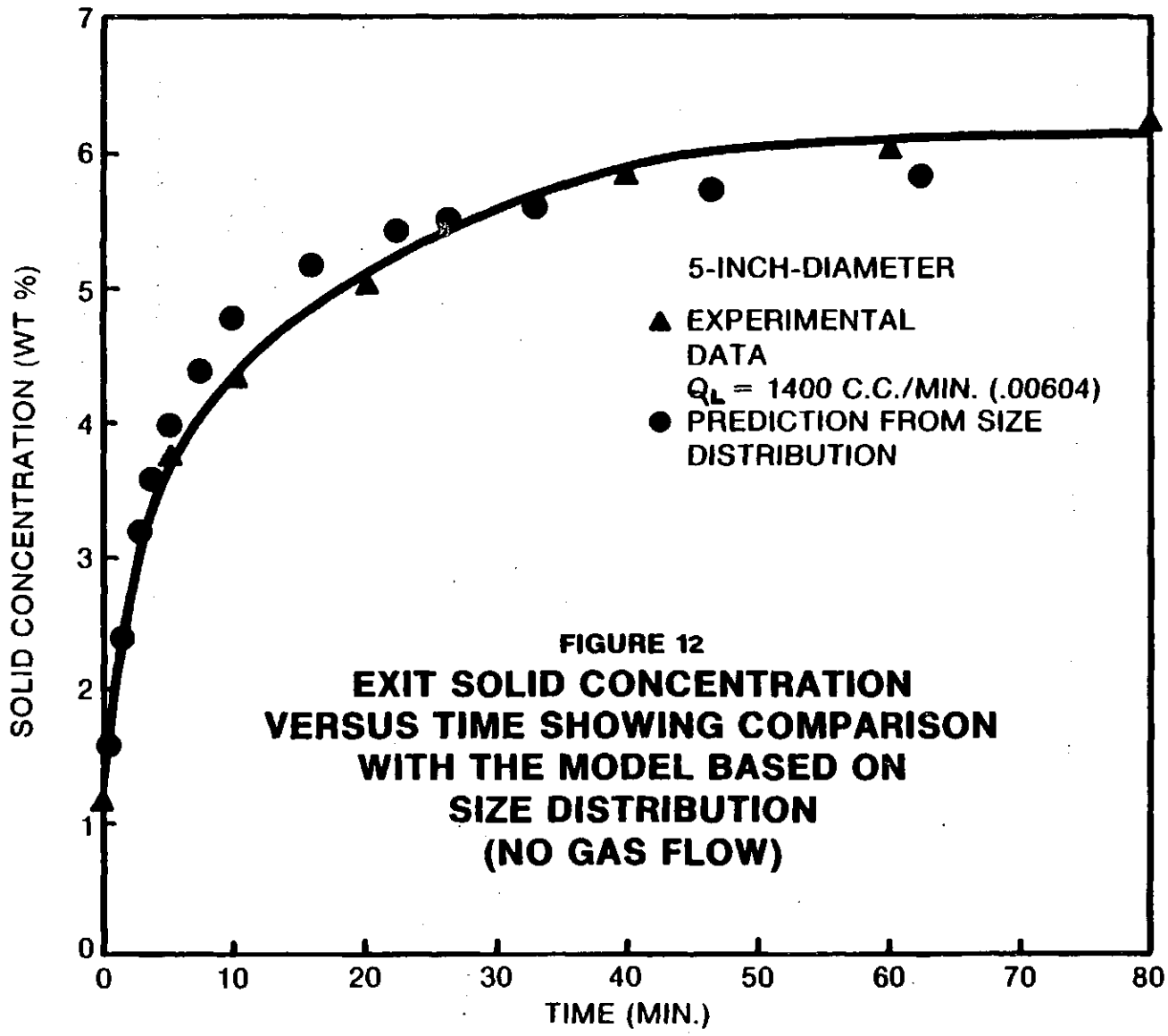

FIGURE 12

EXIT SOLID CONCENTRATION VERSUS TIME SHOWING COMPARISON WITH THE MODEL BASED ON SIZE DISTRIBUTION (NO GAS FLOW)

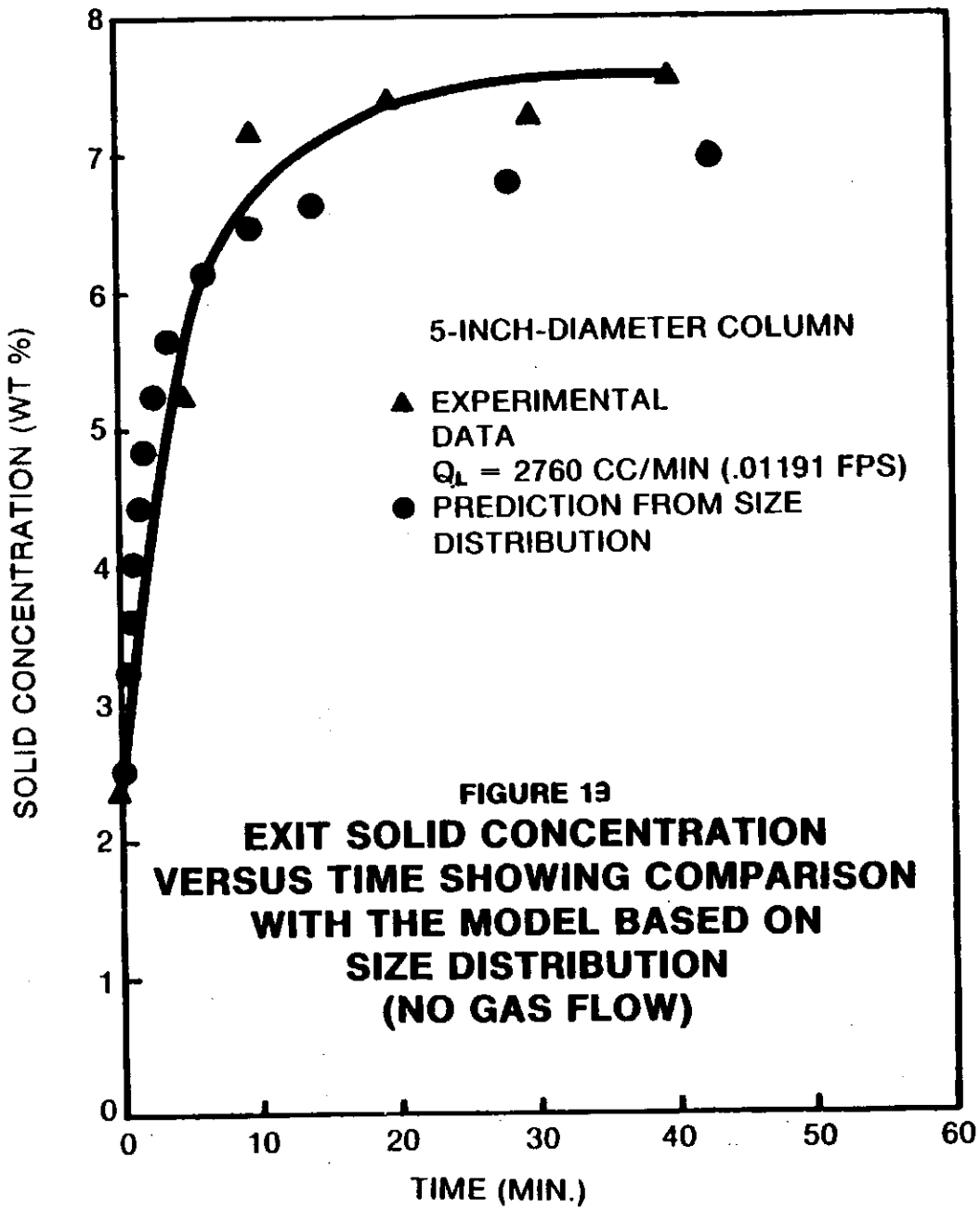

FIGURE 13
EXIT SOLID CONCENTRATION VERSUS TIME SHOWING COMPARISON WITH THE MODEL BASED ON SIZE DISTRIBUTION (NO GAS FLOW)

using particle size distribution and corresponding settling velocity in a later solids accumulation calculation with gas bubbling through the column. The comparison shows that the predicted values are initially slightly higher than the experimental values, but with time the trend reverses. This indicates that the feed may actually have slightly more of the small particles than the size distribution used for the model. When gas was introduced into the system, the effect of slurry flow rate was much less dramatic, although higher exit solids concentration persistently resulted from increasing slurry input rate. The introduction of gas changed the flow system from a plug flow regime to a back-mixing regime, thereby reducing the effect of slurry input rate.

A small amount of gas is sufficient to greatly increase the exit solids concentration. Plots of exit solids concentration versus time at different gas flow rates (constant slurry input) is shown in Figure 14. As can be seen, a more than one order of magnitude increase in the gas input rate did not greatly raise the exit concentration. Since the magnitude of the exit solids concentration can reflect the mixing in the solids phase caused by the gas flow, these results show that solids mixing is greatly enhanced by flowing gas through the column. However, this effect only slightly depends on the gas input rate. The effect of gas flow on solids mixing agrees with the results of a fluid phase mixing study conducted in the 2-in.-diam column. This suggests similar mixing behavior in both the solid and liquid phase of a solid-liquid-gas flow system.

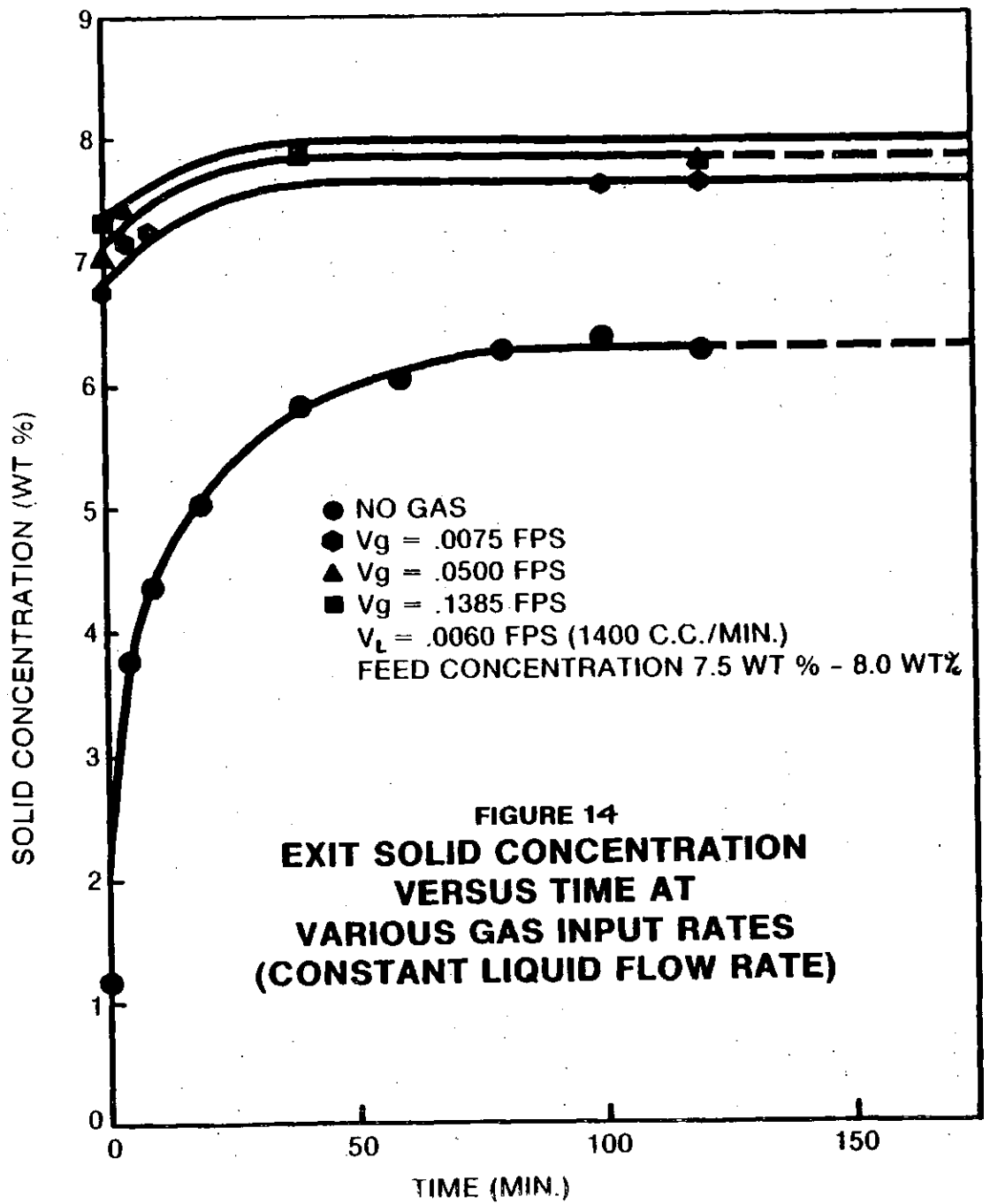

FIGURE 14
EXIT SOLID CONCENTRATION VERSUS TIME AT VARIOUS GAS INPUT RATES (CONSTANT LIQUID FLOW RATE)

A simple but empirical model was used to predict the exit concentration with gas flowing through the column. It was assumed that the exit concentration at time zero was solely due to gas flow and was constant throughout the operating time. A certain fraction of the feed solid would then exit the column constantly as a result of the gas flow. The remaining portion would be carried out by the liquid flow, similar to the case of no gas flow. Comparison of the experimental data with the prediction at two different gas input rates is shown in Figures 15 and 16, indicating a fair agreement. However, poor agreement was obtained at a lower slurry flow rate for the same gas input. Therefore, the more sophisticated model developed by Cova (13) to predict solids concentration as a function of column position and time was used later.

When the results from this study with a water/silica/nitrogen system were extrapolated to the operating times of the Wilsonville dissolver, the predicted value of the retained solids density was much less than that observed at Wilsonville. One factor that could cause the difference in the retained solids density is the possibility of particle agglomeration in Wilsonville's dissolver; this would definitely enhance the amount of retained solid. It was also suspected that the relatively high surface tension of water (72 dynes/cm) would assist exit of the solids from the column, thereby reducing the accumulated solids. However, when the solids accumulation study was carried out in a 30 wt % ethanol-70 wt % water solution to elucidate the surface tension effect, the retained solids density in the solution was even slightly less than that in water. Therefore, the observed high retained solids density in the Wilsonville dissolver may be attributed to the particle agglomeration.

FIGURE 15

EXIT SOLID CONCENTRATION VERSUS TIME SHOWING COMPARISON WITH THE MODEL FOR LOW GAS FLOW RATE

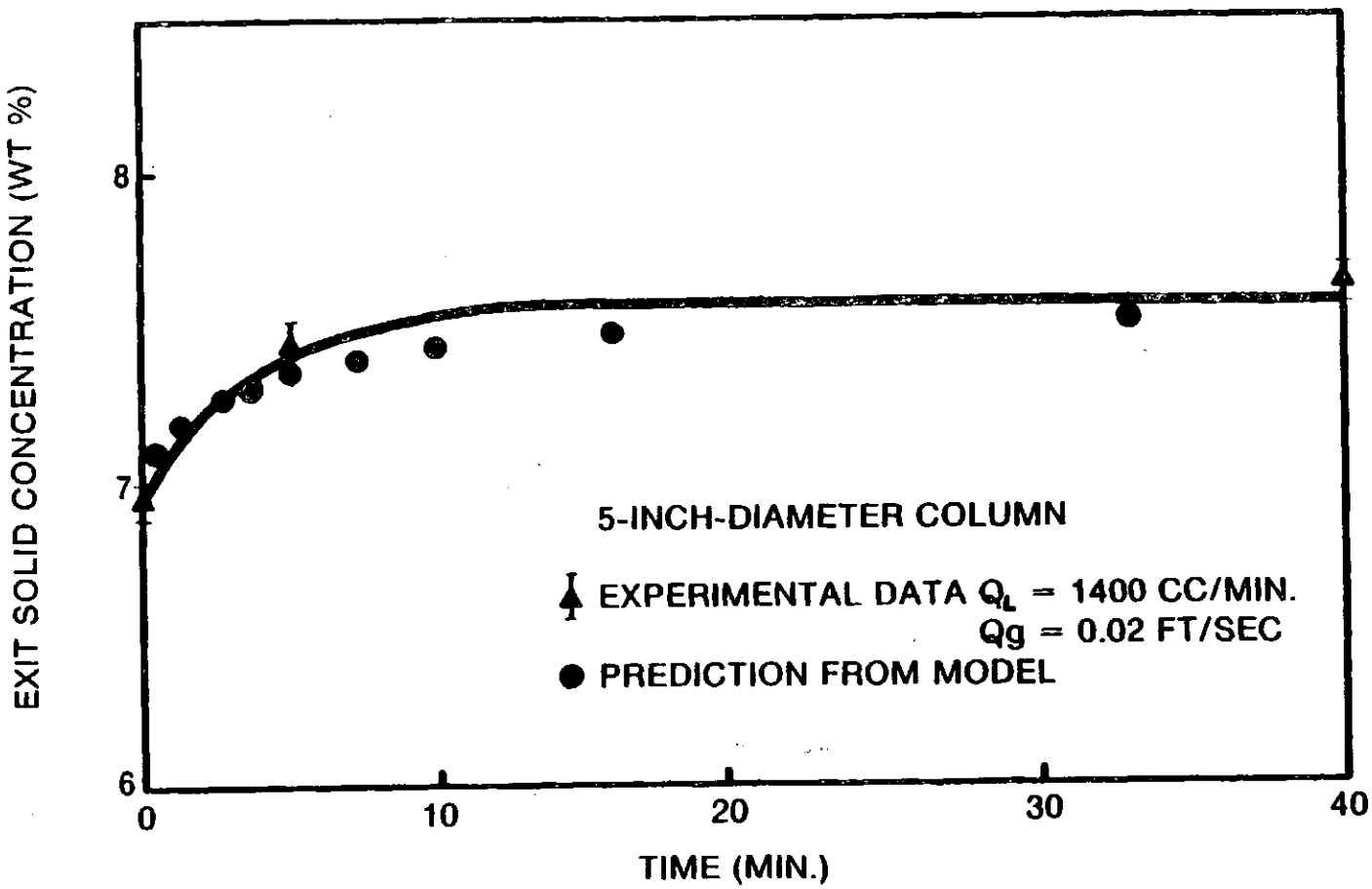

FIGURE 16

EXIT SOLID CONCENTRATION VERSUS TIME SHOWING COMPARISON WITH THE MODEL FOR HIGH GAS FLOW RATE

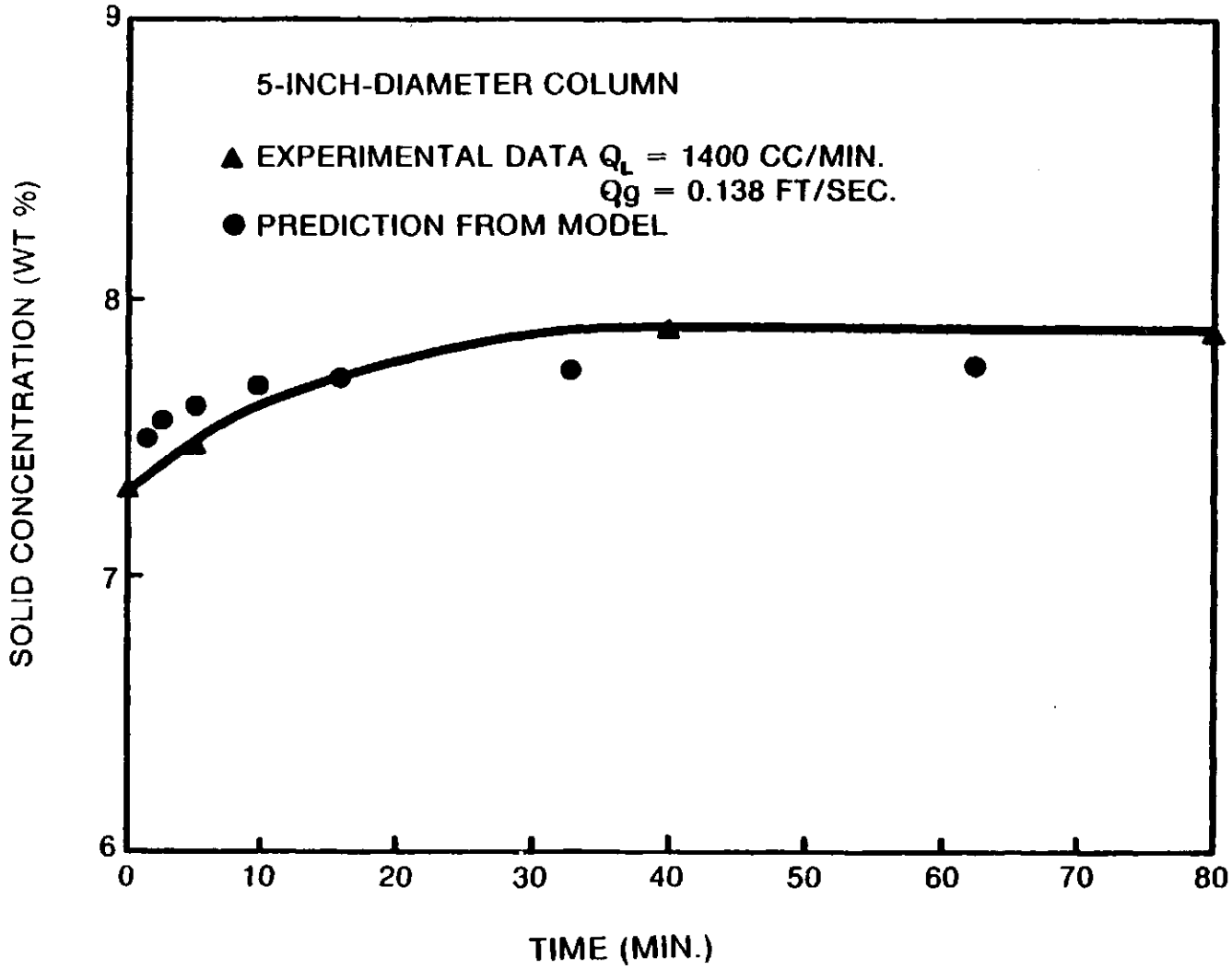

The solids accumulation model employing diffusion superimposed on bulk flow was used to determine the axial dispersion coefficient for the 5-in.-i.d. column. Diffusivity was the sole adjustable parameter to fit the solids distribution data; a value between 0.08 and 0.10 ft^2/sec was found to best fit the data, as shown in Figure 17. This experimentally determined value of axial dispersion coefficient agreed very well with the prediction from six different correlations. Most of the predicted value range (0.088-0.133 ft^2/sec) was slightly higher than the experimental value range (0.08-0.10 ft^2/sec).

Dispersion of the Liquid Phase

A tracer detection method was employed to determine the degree of dispersion in a column of nitrogen gas bubbling through water. The conductivity-versus-time plot was transformed into a dimensionless tracer curve, which was then fitted to the axial dispersion model for which the Peclet number (VL/E_z) was the sole fitting parameter. The dispersion coefficient or diffusivity in the liquid phase was calculated from the Peclet number.

At the SRC-I Demonstration Plant design gas and liquid velocity (0.33 and 0.05 ft/sec, respectively), a dispersion coefficient of 0.1842 ft^2/sec was found. This experimentally determined value was compared with the dispersion coefficients calculated from six correlations published in the literature, and an excellent agreement was observed with five of them. In general, the experimentally determined values were less than the prediction from the five correlations.

FIGURE 17

SOLID CONCENTRATION DISTRIBUTION VERSUS COLUMN HEIGHT SHOWING COMPARISON WITH THE MODEL BASED ON DIFFUSION SUPERIMPOSED ON BULK FLOW

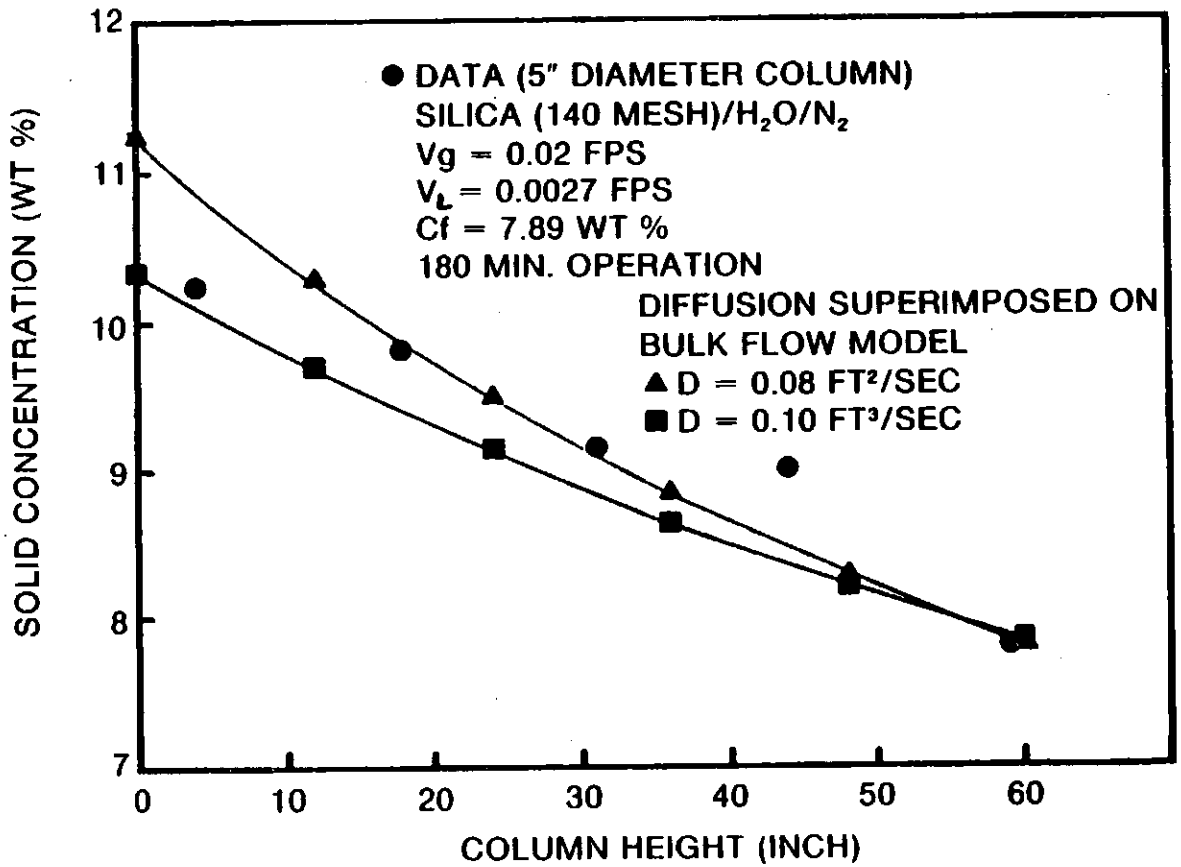

The dispersion coefficient was found to be independent of liquid velocity; this agrees with the conclusion of most other investigators. With an almost tenfold increase in the superficial water velocity from 0.0061 to 0.05 ft/sec at a constant gas superficial velocity of 0.09 ft/sec, the experimentally determined value for the axial dispersion coefficient was 0.1014 ft^2/sec. This value agreed very well with the same five correlations and is slightly lower than the predicted values.

The axial dispersion coefficients were calculated from the tracer curves obtained from both the 2- and 5-in.-i.d. columns at different gas and liquid velocities. Using dimensional analysis, a correlation was developed as shown below:

$$\frac{E_z}{D\ V_G} = k\left(\frac{Dg}{V_G^2}\right)^n \tag{8}$$

The empirical parameters k and n were determined to be 0.27 and 0.32, respectively. An explicit expression for the dispersion coefficient was obtained as follows:

$$E_z = 0.27\ g^{0.32}\ D^{1.32}\ V_G^{0.36} \tag{9}$$

Because the presence of solid particles reduces dispersion in the liquid phase, the 5-in.-i.d. column was filled with 30-45 mesh sand particles to an average solids concentration of 16 wt %. Water flowed at a velocity of 0.05 ft/sec, and the experiments were performed at different gas velocities. In all cases, the calculated dispersion coefficient was less than that obtained in the absence of solid particles, as shown below:

Effect of Solid Particles on Dispersion Coefficient

V_{water} = 0.05 ft/sec
Solids concentration = 16 wt %, 30-45 mesh sand

V_{N_2} (ft/sec)	E_z without solid (ft^2/sec)	E_z with solid (ft^2/sec)
0.02	0.0663	0.0442
0.09	0.0909	0.0614
0.33	0.1842	0.0814

The percentage of reduction in E_z (33%) is the same at low gas velocities of 0.02 and 0.09 ft/sec, but the reduction (56%) increases at a higher gas velocity of 0.33 ft/sec. The overall impact of the reduction in the dispersion coefficient due to the presence of solids is that it greatly reduces the degree of mixing of the system.

CPDU Reactor Simulation

A large number of trace curves, solid concentration distribution profiles, and dispersion studies were carried out with the 2-in.-i.d. column during the CPDU reactor simulation studies. These studies became the basis for the additional studies conducted in the 5-in.-i.d. column, the results of which were presented in this report. However, it is of interest to note the main conclusions arrived at from the initial simulation work:

- The dispersion model can be applied to this system (simulator) if stagnant or semistagnant regions do not exist.

- Liquid mixing to suspend solids is mainly caused by gas bubbles.

- At constant gas flow, mixing decreases as liquid flow increases.

- Distribution of solids in the reactor is a function of gas velocity through its dependence on the axial dispersion coefficient.

- The particle distribution profile within the reactor may be essential to the heat transfer design since the solid particles catalyze the hydrogenation reaction.